MINIATURE CONDUCTIVE POLYMER ACTUATORS FOR HIGH PRESSURE GENERATION IN LAB ON CHIP SYSTEMS

M. Hiraoka[1,2] P. Fiorini[2], J. O'Callaghan[2], I. Yamashita[1], C. Van Hoof[2], M. Op de Beeck[2]
[1]Advanced Technology Research Laboratories, Panasonic Corp., Kyoto, Japan,
[2]imec, Kapeldreef 75, 3001 Leuven, Belgium

ABSTRACT

We developed a miniaturized 'syringe type' pump (8 mm diameter, 1 mm thickness) which generates a flow rate of 2 μL/min at a pressure of 3 MPa. It consists of a stack of several conductive polymer (CP) layers intercalated with electrolyte layers. The stack is housed in a polycarbonate case specially conceived for integration in a lab-on-chip device. The dependence of strain on applied bias is investigated and the optimum working condition is determined. The actuator operates at a bias lower than 2V. A maximum strain of 13% is measured in the single CP layer when it expands against atmospheric pressure; this strain is reduced by only a factor of 3 when pressure increases up to 15 MPa. The power efficiency of the actuator is also measured; it is in the range 10^{-3}-10^{-4} and increases when pressure increases. Using a stacked actuator, consisting of 8 single actuators stacked on top of each other, a maximum strain of 5% is measured against atmospheric pressure.

1. INTRODUCTION

Micropumps are key components in microfluidic systems, having the function of moving small volumes of chemical and biological liquid. Two main groups of micropumps exist: reciprocating and dynamic pumps [1]. Dynamic micropumps directly transfer to the fluid the energy necessary for its motion without the use of moving parts. A multitude of actuation mechanism has been used, such as magnetohydrodynamic, electrohydrodynamic, and electro-osmotic actuation. Reciprocating micropumps on the other hand, always include solid moving parts. Diaphragm-type micropumps, usually driven by piezoelectric actuators, are the most common example of this category.

Examples of high pressure applications (up to a few MPa) are pressure driven electrophoresis and chromatography, commonly used in the biomedical field. Their integration in Lab on Chip (LoC) devices calls for the development of miniaturized, high pressure pumps. Among the dynamic micropumps, electroosmotic pumps generate large pressures [2]. Unfortunately they require a large driving voltage, in the KV range. The choice of reciprocating micropumps is in this case preferred. Only a few types of actuators can generate pressure in the MPa range, examples are gel actuators, shape memory alloys and conductive polymers [3]. Gel actuators are generally very slow, operation is frequently unstable and the gel must be confined in a closed space. Shape memory alloy based actuators must be cycled between two temperatures, a condition which is often inconvenient. A thermally activated, high pressure (15 MPa) micropump has been demonstrated [4]; thus being operated at low voltage its power consumption is very large (1-2 W). In a recent paper [5] Hiraoka et al. described a syringe type pump, based on a conductive polymer (CP) actuator. The actuator, which has no major drawbacks, can be easily fabricated and generates the required large pressures. Furthermore it can be driven at low voltages, less than 2 V. As power consumption is low, it can operated by a small battery, thus allowing its use in portable devices. In this paper we report an extended characterization of the actuator and the pump demonstrated in [5]. Section 2 is devoted to the actuator itself; principle of operation, fabrication method and characterization are discussed. Section 3 concerns the coupling of the actuator to a fluidic chip in order to generate a flow against a large back pressure. Conclusions are drawn in section 4.

2. CONDUCTIVE POLYMER ACTUATOR

2.1 Operation Principle

CP actuators transform electrical energy into mechanical energy. The operation principle of a CP actuator is schematically illustrated in Fig.1a: ions in the electrolyte are injected in or extracted from the CP upon application of negative or positive bias, causing a volume change of the CP film. The ions are attached to the polymer chains by Coulomb forces and no strong covalent bond is formed, enabling cyclic operation of the actuator (Fig. 1b). The number of cycles which occurs without performance degradation depends on the applied bias; if bias is kept relatively low millions of cycles can be performed. To the contrary, if large voltages are applied in order to reach maximum displacement, the number of useful cycles decreases to a few thousands or less [6]. The fact that performances might degrade with increasing cycle number does not hinder the use of these actuators in disposable lab-on chip.
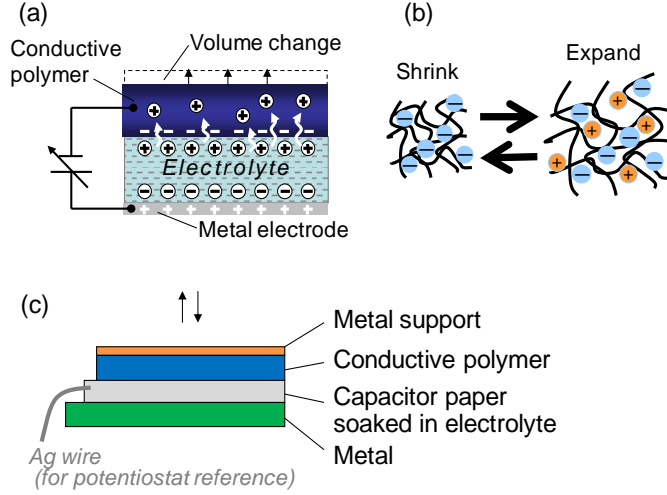
Fig. 1: Operating principle of the CP actuator. (a) Electrical circuit for actuator operation. (b) Microscopic representation of a shrinking/expanding cycle. (c) Stack of layers used for polymer characterization. In some cases the bottom metal is replaced by an inactive CP layer.

As the working principle of CP is based on ion diffusion, the actuator is inherently slow; furthermore velocity gradually decreases while the actuator approaches the maximum displacement. In order to obtain large displacement in a short time a stacked actuator is used: several individual thin actuators are stacked on top of each other and operated together.

The most common CP actuators exploit bending beam motion or in-plane deformation, we realized actuation by modulation of film thickness, hence out-of-plane actuation, as also reported in [7]. In this configuration the generated force is much larger.

2.2 Preparation

The fabricated actuators are based on Polypyrrole Bis (trifluoromethyl- sulfonyl)imide, further referred to as PPy-TFSI, a CP recently proposed in literature [8]. A non volatile ionic liquid, 1-ethyl-3-methyl-imidazolium (EMI)-TFSI was used as electrolyte. This electrolyte combined with PPy gives large displacement, long cycle life, stable and repeatable displacement [9]. For comparison purposes, we also synthesized and studied polypyrrole dodecylbenzene –sulfonate (PPy-DBS), a more common CP.

The base material for the actuator is polypyrrole (PPy). It is prepared by electrolytic polymerization from a pyrrole (Py) solution at room temperature. A silicon wafer coated with TiW-Pt is used as anode. The cathode is a Pt black electrode placed in front of the anode at about 5 mm distance. Different types of negative doping ions A^- can be added to the Py solution during deposition. Polymerization and ion inclusion are regulated by the following reaction:

$$n\mathrm{PyH}_2 + A^- \rightarrow (\mathrm{Py})_n^+ A^- + 2n\mathrm{H}^+ + (2n+1)e^- \tag{1}$$

were PyH_2 is a pyrrole monomer, (the side groups of hydrogen which are removed during polymerization are explicitly written as H_2). The value of n is known to be between 2 and 3. Electrical and mechanical properties of the polymer depend on the added ion A^-, as already mentioned TFSI or DBS are used as dopant ions in this work. The fabrication of stacked actuators requires that the individual layers have smooth surfaces, hence polymerization parameters such as solution molarity, solvent type and current density have been adjusted taking also this requirement into account and not only aiming at maximum force and strain. Indeed, larger values of force and strain than those reported in this paper have been observed in PPy-TFSI [10] but in that case the surface of the polymer is extremely rough, hence the material is not suited for the fabrication of stacked actuators.

Table I summarizes the deposition parameters of the investigated material, conventional names used through this paper to

Table I: Material deposition parameters: conventional name, dopant ion, solute, solvent , anodization current I, deposition time t, obtained film thickness h, normalized deposition rate u and electrical conductivity σ along in-plane direction.

Name used in this paper	Ion	Solute	Solvent	I [mA/cm^2]	t [min]	h [μm]	u [μm cm^2/C]	σ [S/cm]
TFSI(IL)	TFSI	0.2M Py	EMI TSFI	0.7	200	70	8.3	2
TFSI(MB)	TFSI	0.2M Py 0.2M EMI-TSFI	Methyl benzoate	1	180	60	5.6	15
DBS	DBS	0.1M Py 0.1M Na-DBS	D. I. Water	1	43	15	5.8	7

identify the various material are also reported. Notice that two types of electrochemical baths have been used for preparing PPy-TFSI. Some interesting comments can be made when looking at the values listed in Table I. Since DBS ions are larger than TFSI ions, the deposition rate u of PPy-DBS is expected to be larger than that of PPy-TFSI. Our experiments show that this is not the case, indicating that PPy-TFSI is a more porous material than PPy-DBS, in accordance with [10]. This porosity is further confirmed by the fact that PPy-TFSI films were swelling up to ~150% of their original volume when soaked in acetone, an effect not observed for PPy-DBS. Similarly, we believe that the difference in deposition rates u for PPy-TFSI (IL) and PPy-TFSI (MB) indicates that the first material is more porous than the second. Another comment relates to the electrical conductivities σ. The σ-values reported in Table I are lower than state-of-the-art ones, due to the fact that we performed electrochemical synthesis at room temperature and not close to the melting temperature of the solvent, as usually done and reported in literature. We prefer a room temperature process since it will strongly facilitate the transfer to an industrial environment. As proved by the functionality of the stacked actuator, the obtained conductivity values are perfectly suited for the targeted application.

2.3 Characterization

We investigated the vertical displacement of the materials listed in Table I upon bias application, using the test structure shown in Fig. 1c. It consists of: (i) a bottom electrode, referred to as counter electrode (CE), (ii) an electrolyte layer made of paper soaked in electrolyte and connected to a silver wire acting as reference electrode (RE), and (iii) the conductive polymer under investigation. The bottom electrode is sometimes made of a silicon piece covered by a TiW adhesion layer and finished with platinum. More often the Pt bottom electrode is replaced by a CP layer which does not expand or contract with the used electrolyte. We will refer to this layer as the inactive CP. As for the electrolyte, in the case of PPy-DBS we used either a 0.1 M NaCl aqueous solution, as previously reported in the literature [7], or EMI-TSFI, while in the case of PPy-TFSI only EMI-TFSI was used. As for the top contact, indicated as working electrode (WE), a rigid metal layer was deposited on one side of the CP. This layer has a double function: confining the volume change of the CP only to the out-of-plane direction and avoiding excessive lateral potential drops in CP film during electrochemical reaction [11]. The metal layer was realized by sputtering an adhesion layer of 20 nm TiW followed by an electron beam deposition of 150 nm Au. Deposition rate was 0.7nm/s for both layers. Prior to this metal deposition the CP layer was rinsed in the pure solvent used for polymerization and carefully dried. Bias is typically supplied to the CP actuator by means of a potentiostat, which allows setting the voltage drop between the electrolyte (reference electrode) and the working electrode. The bias reported in the figures and referred to in the text is this potential difference, unless explicitly indicated.

Two types of characterization have been performed, in one case the actuators expands basically against atmospheric pressure, in the other case it expands against a large pressure (up to 15 MPa).

2.3.1 Actuator characterization using a small load

Vertical displacement was measured in case of expansion of the actuator against a low pressure (0.1 MPa). A small weight and a mirror are placed on the stack of Fig. 1c, and the specimen is positioned on the stage of a laser displacement sensor (Polytec LDV PSV-400). Typical experimental curves of the displacement as a function of the applied bias are reported in Fig. 2. In these measurements a platinum counter electrode is used. At start, a negative bias voltage is applied and the actuator expands, then bias is reversed to a positive one and the actuator contracts. The value of the strain after 60 s of negative bias application versus bias itself is reported in the inset of Fig. 2. A curve, which is just an eye guideline, is drawn through the experimental points.
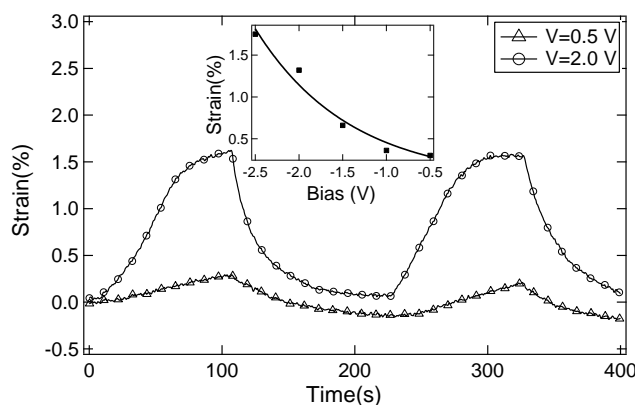

Fig. 2: Behavior of strain as a function of time for different applied bias. Bias is negative when the actuator expands (e.g. from 0 to 100 s) and positive when the actuator contracts (e.g. 100 to 200s). The inset indicates the behavior of displacement as a

function of applied bias.

We notice that when the applied voltage approaches large negative values the displacement increases more rapidly. In this region the actuator becomes unstable and the displacement reduces noticeably from one cycle to the following one. The raise time of the strain depends on applied bias and on the ion diffusion coefficient. At low applied bias, the expansion rate is limited by the low speed of the chemical reaction: after 100 s only a fraction of the ions which can be accommodated in the CP has been injected, we can state that raise time is definitely longer than 100 s. At large applied bias, the expansion rate is limited by the diffusion of ions through the CP layer. In the specific case of an applied bias of 2V, shown in Fig.2, saturation occurs after about 80 s, which roughly corresponds to the time ions need to travel through the thickness of the CP layer. The corresponding diffusion constant is $\sim 10^{-7}$ cm^2/s which is consistent with previous literature results [12].

Strain measurements for different materials, partly obtained in this work, partly from literature, are reported in Fig. 3. Data show that the PPy-TFSI synthesized from EMI-TSFI solutions and developed in this work outperforms PPy-DBS, previously used for the same type of actuators [7]: strain remains constant with increasing film thickness. A maximum strain of 13% is obtained. The displacement of both PPy-TFSI (MB) and PPy-DBS operated in EMI-TFSI is smaller than that of PPy-TFSI (IL).
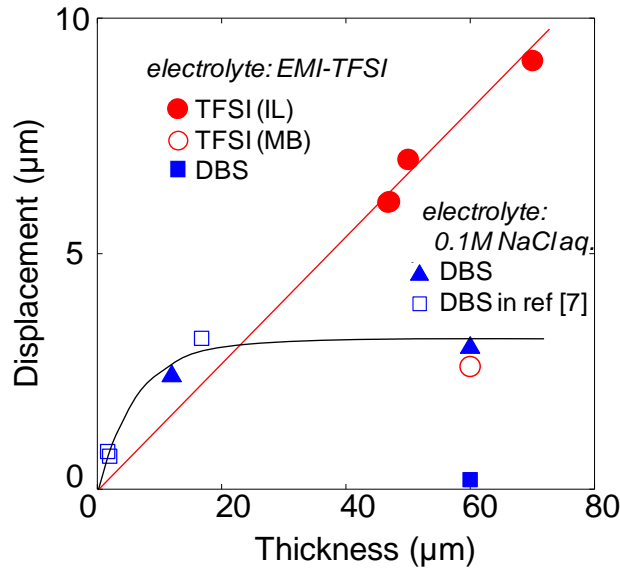

Fig 3: Dependence of the displacement on CP layer thickness for PPy-DBS and for PPy-TFSI. The red line refers to PPy-TFSI(IL) operated in EMI-TFSI, the black line to PPy-DBS operated in aqueous solution. Lines are just eye guides.

Fig. 4 shows the dependence of displacement, of charge and of their ratio vs. time. Fig. 4a refers to PPy-TFSI(IL) and Fig. 4b to PPy-TFSI(MB). In both cases EMI-TFSI is used as electrolyte. To start, a negative bias voltage is applied and it is reversed to a positive bias after 100 s. The charge density Q accumulated in the layer at t = 100s is 0.4 C/cm^2 for PPy-TFSI (IL) and 0.3 C/cm^2 for PPy-TFSI (MB). The ratio $\gamma = Q/e$ (in cm^{-2}) represents the surface density of Py sites in the CP layer which reacted with the ions injected from the electrolyte. From equation (1), the total Py surface density N in the CP film can be written as:

$N = Q_0 n/(2n+1)e$ (2)

where Q_0 is the total charge passed during electrolytic polymerization, i.e. $Q_0 = h/u$ (C/cm^2) (*u* and *h* as listed in Table I). From γ and *N*, we can estimate the percentage β of Py-sites which reacted with electrolyte ions in the CP film during actuator operation. Indeed, we have:

$\beta = \gamma/N = Q(2n+1)/Q_0 n$ (3)

Assuming $n = 3$, $\beta \sim 2.3 Q/Q_0$ and hence β is estimated to be 11% and 6%, for PPy-TFSI (IL) and PPy-TFSI (MB) respectively. This calculation suggests that the effective surface available for electrochemical reaction in PPy-TFSI (IL) is twice as large as in PPy-TFSI (MB), which explains the difference in displacement shown in Fig. 4 a and 4b.

The same type of analysis can be carried on for PPy-DBS, resulting in $\beta = 2.7$ %. In spite of this value, which is only half of the one measured for PPy-TFSI(MB), no displacement is measured (see Fig. 3). The reason for this behavior is not clear, and deserves further work. In this work we have used PPy-DBS as an inactive counter electrode for pump fabrication, replacing the expensive Pt electrode.
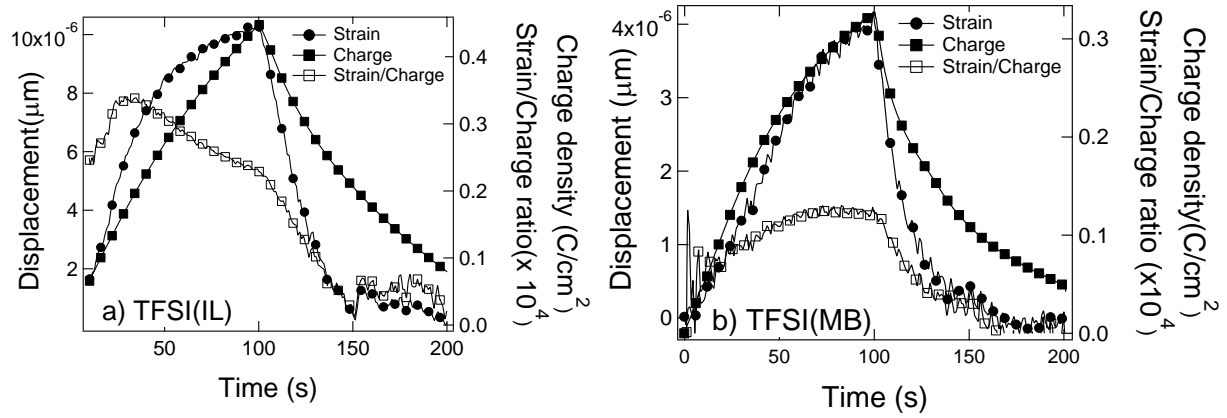
Fig.4: a) refer to TFSI(IL) and b) to TFSI(MB). Note that scales are different. In each figure the displacement (left axis), the charge accumulated in the CP layer during operation (right axis) and the displacement to charge ratio (right axis) are reported vs. time. Negative voltage is switched on at t =0 s, voltage is reversed at t = 100 s. Negative and positive voltages are -1.4V/+1.0V for PPy-TFSI(IL) and -1.5V/+1.2V for PPy-TFSI(MB) .

It is interesting to analyze the behavior of the displacement-to-charge ratio, i.e. of the charge conversion efficiency reported in Fig. 4. First we notice that it is lower for TFSI(MB) than for TFSI(IL). This is a consequence of the fact that values of □ for the two materials are different as discussed before. Second we observe that the displacement/charge ratio is dependent on time, and this dependency is different for the two materials. In order to interpret this behavior, we recall two well know facts: i) in the case of in-plane strain operation [12], where thin layers of CP are used, displacement and charge are exactly proportional, hence strain/charge is a constant, ii) when thick layers of CP are deposited, properties such as density and rigidity gradually vary along the growth direction. These two facts suggest that the time dependent behavior of charge conversion efficiency just maps the spatial non-uniformity of the CP films. To be more precise, we can interpret the initial increase, observed for both materials, as a consequence of the fact that voids and defects are present in the top layers of the CP. The fact that in the case of TFSI(MB) the charge conversion efficiency saturates suggests a larger grade of material uniformity than in the case of TFSI(IL) where charge conversion efficiency decreases with time (except for the initial phase).

In the characterization presented until now measurements have been performed by means of a potentiostat which is measuring the voltage drop between the electrolyte and the CP. The potential difference between the reference and the working electrode (WE) has been considered as the independent variable. In real applications another working mode will be used: bias will be applied between the WE and the counter electrode (CE) and there will be no possibility to monitor or fix the voltage drop between the electrolyte and the CP. For this reason we have compared the behavior of the actuator when biased in the two modes described above. Results are reported in Fig. 5 and refer to an actuator where the counter electrode is made of PPy-DBS, i.e. of an inactive CP. It is worth to notice that the areas of the WE and of the CE are in this case identical.
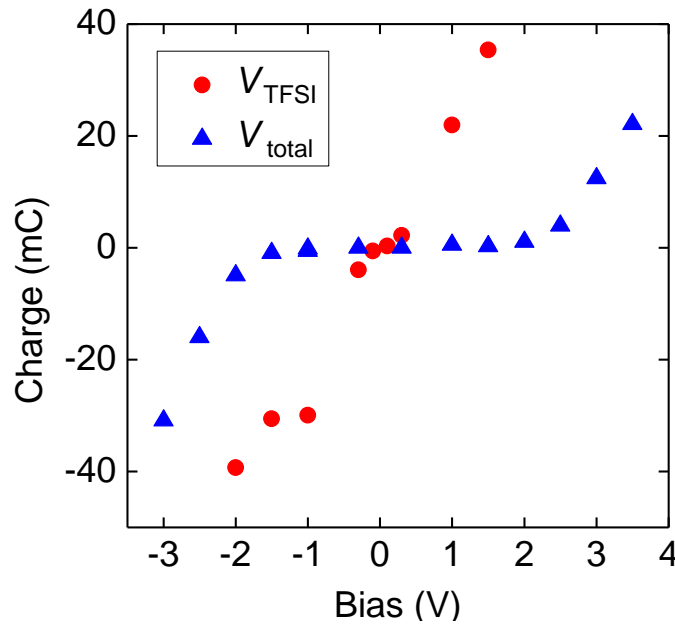
Fig. 5 Behavior of the charge as a function of applied bias for a TFSI(IL) actuator. Circles: voltage drop between the working and reference electrode. Triangles: voltage drop between the working and the counter electrode.

We notice that when a positive bias of 3.7 volts is applied between the CE and the WE (triangles in the Fig. 5), the accumulated charge is about 28 mC. Potentiostat measurements (circles in fig. 5) indicate that this charge is obtained when a bias of 1.2 volts is applied across the electrolyte/TSFI interface. This means that the voltage drop between the electrolyte and the CE is 2.5 V, this is a fairly large value which causes instabilities in the PPy-DBS counter electrode. We believe that this is at present the limiting factor of the actuator performance: a better engineering of the CE might allow applying a larger voltage between the electrolyte and the working electrode obtaining faster and/or larger displacement.

2.3.2 Actuator characterization using a heavy load

Strain measurements against a loaded spring system (performed by adapting a delaminator tool from DTS) show that cyclic operation is possible also at very high pressure (Fig. 6a) since repeatable strain versus time curves are observed.
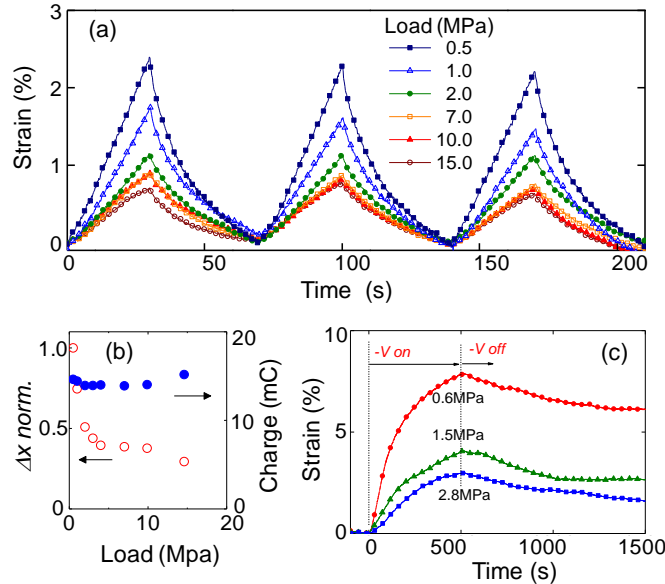

Fig.6: (a) Time dependence of strain for different loads applied to the actuator. Voltage is cycled between +1.2V and -1.6V. (b) Left axis: Dependence of strain on pressure. Data are normalized to atmospheric pressure expansion. Right axis: Charge difference at half cycle. (c) Time dependence of strain when bias is applied for 500 s and then switched off.

Furthermore the experiments prove that strain is reduced by only a factor of 3 when pressure increases from 0.5 MPa to very high pressures such as 15 MPa, (first and last red data points in Fig. 6b). We can see that the dependence of normalized displacement is not linear. It can be decomposed in two linear behaviors, one corresponding to a blocking pressure of 5 MPa and the other to a blocking pressure of 30 MPa. Again this behavior is different from the one observed in the case of in-plane strain, where the dependence is linear [6]. The non linearity of the displacement vs. pressure curve might be due to pressure dependence of charge injection or to non-homogeneous structure of the CP. We verified that charge is basically pressure independent (see Fig. 6b), hence we believe that the origin of the non linearity resides in a non homogeneous polymer structure, as discussed before in relation to Fig. 4. To be more clear, this means that Fig. 6b can be roughly interpreted by assuming that the CP layer is made of two layers, one characterized by a low blocking pressure (7-10 MPa), the other by a large blocking pressure (~30 MPa). Fig. 6c shows the strain behavior when bias is applied for a long time, 500 s, and then removed. In open circuit condition the strain decreases very slowly with time; this opens the possibility of using this material also for valve fabrication.

An important figure of merit of actuators is their energy efficiency, which is the ratio between the mechanical work done by the pump, and the electrical energy transferred to the pump. The dependence of this efficiency on pressure can be determined from the data of Fig. 6a. The electrical energy is just the electrical power multiplied by the time. The mechanical work is the sum of two contributions: (1) the elastic energy accumulated in the actuator during expansion and (2) the energy due to the displacement of the actuator surface against the applied pressure. In the explored range of pressure the first contribution is always negligible. Efficiency ranges from $4 \cdot 10^{-4}$ at a pressure of 0.5 MPa to $3.2 \cdot 10^{-3}$ at a pressure of 15 MPa. These efficiency values are typical of conductive polymers.

3 PUMP FABRICATION

As the diffusion rate of ions in CP is low, $\sim10^{-7}$ cm^2/s, large displacements should not be obtained by increasing the thickness of the polymer layer beyond ~100 μm, this would increase too much the response time. The solution proposed here consists in fabricating a stacked actuator, schematically shown in Fig. 7a. The actuator is made by stacking several base units, each comprising a PPy-TFSI film as the active part, a capacitor paper soaked in EMI-TFSI as the electrolyte and a PPy-DBS layer as passive counter electrode. The thicknesses of the various layers are respectively ~70 μm, 33 μm and ~20 μm. The total thickness of a 8 units stacked actuator is then 960 μm of which ~560 μm is active CP material. In the case of 13% of strain in each of the 8 PPy-TFSI layers, a total displacement of 70 μm is expected. We notice here that in the fabrication of the stacked actuator the single layers are taken from the same sheet. This means that they have been deposited together and hence have a very uniform behavior.

The electrical connections between the various layers are made by a silver wire inserted into dedicated holes in the layers and fixed with silver paste. The stacked actuator is manually placed in a 830 μm thick polycarbonate case closed at the bottom by a 25 μm thick polyimide (PI) membrane. The PI membrane is attached to the polycarbonate case by a 10 μm thick glue layer (Loctite3211) patterned on the PI itself by automated screen printing. The polycarbonate case is sealed by gluing a thin glass plate at the top. The thickness of the glue used to connect these two elements, is tuned in such a way that the bottom part of actuator ends at a distance $\Delta h \sim100$ μm below the bottom part of the polycarbonate case (see Fig. 7a). Because of the tension T in the PI (Fig. 7a), a vertical force is generated, which prevents the separation of the individual layers during operation. The tension T was measured and is about ~200 mN, which corresponds to a pressure of ~10 kPa on the bottom of the actuator. The length of the PI stretched region is about 1.5 mm, and for $\Delta h = 100$ μm the strain in the PI is about 0.2 %. During cyclic operation of the actuator, the value of Δh is almost doubled; corresponding to 0.5% strain of the PI, which is still below the 1% limit where irreversible deformation of PI film occurs. Therefore PI stretch motion is reproducible during pump operation. The packaged actuator is glued (by Araldite) on a micro-fluidic system as shown in Fig. 7b and 7c.

The structure shown in Fig. 7a has been characterized by measuring the displacement with the same tools and techniques used for the single actuator layer. Results are reported in Fig. 8a. The obtained displacement is close to 30 μm, which corresponds to a strain of 5%, which is more than 2 times smaller than the strain obtained with single layers.
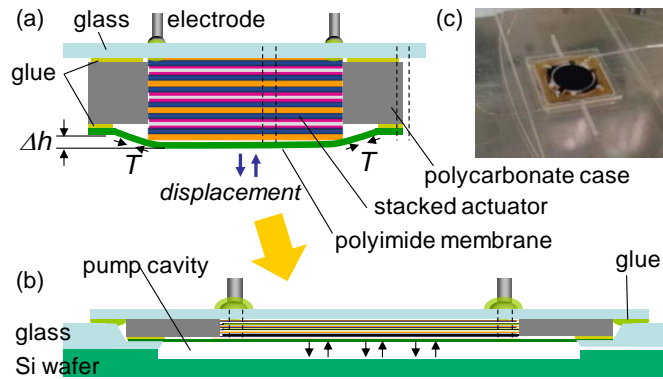
Fig.7: (a) Schematics of the packaged actuator. (b) The packaged actuator is glued to a micro-fluidic system, so as to form a variable volume cavity. (c) Photograph of the packaged actuator mounted on a fluidic structure.

This strain reduction is due to the presence of voids between the layers, and can be limited by more accurate mounting. The outer left axis in Fig. 8a is the expected volume change of the pump cavity shown in Fig.7. It can be easily evaluated from the displacement vs. time data and from the actuator diameter. The initial flow rate, i.e. the change in volume per unit time just after bias application, is 4.7 μL/min.

Fig. 8b shows that the dependence of strain on pressure for the stacked actuator closely parallels the one of the single layer actuator in Fig. 6b. The initial flow rate reduces to ~2 μL/min at 3 MPa.
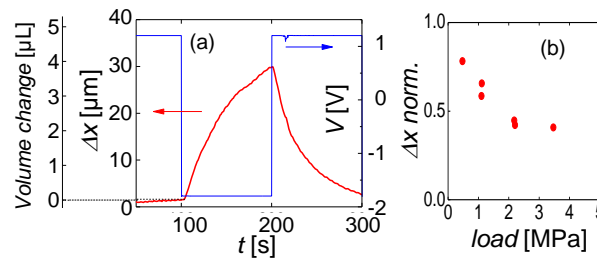

Fig8: (a) Displacement and applied bias vs. time for a packaged actuator. The outer left axis is the expected volume change of the pump cavity. (b) Dependence of displacement on pressure. Data are normalized to atmospheric pressure expansion.

4 CONCLUSIONS

We have reported for the first time the successful fabrication of stacked actuators based on the conductive polymer PPy-TFSI. Actuator characterization showed very good results: a displacement of 30 μm and a blocking pressure of 30 MPa have been demonstrated. Operation voltage is below 2 V. The actuator has been integrated in a simple micro-fluidic system, so as to act as a pump, thus demonstrating its suitability for autonomous LoC devices.

REFERENCES

[1] D. J. Laser and J. G. Santiago, A review of micropumps, J. Micromech. Microeng. 14 (2004) R35–R64

[2] Z. Chen, P. Wang, and H. Chang, An electro-osmotic micro-pump based on monolithic silica for micro-flow analyses and electro-sprays, Anal. Bioanal. Chem. 382 (2005) 817–824

[3] S. Wilson, New materials for micro-scale sensors and actuators an engineering review, Mat. Sci. Engin.-R 56 (2007) 1-129.

[4] Stefan Svensson, Gunjana Sharma, Sam Ogden, Klas Hjort, and Lena Klintberg, High-Pressure Peristaltic Membrane Micropump With Temperature Control, J. of MEMS 19, (2010) 1462.

[5] M. Hiraoka, P. Fiorini, I. Yamashita, C. Van Hoof, M. Op de Beeck, High pressure pump as lab on chip component for micro-fluidic integrated system, IEEE 24th International Conference on Micro Electro Mechanical Systems (2011) 1139-1142

[6] W. Lu, A.G. Fadeev, B.Qi,E. Smela,B.R. Mattes, J.Ding, G.M. Spinks, J. MazurkieWicz, D. Zohu, G.G. Wallace, D.R. MacFerlane, S.A. Forsyth, M. Forsyth, Use of ionic liquids for pi-conjugated polymer electrochemical devices, Science. 297(2002) 983-987

[7] E. Smela and N. Gadegaard, Volume change in polypyrrole studied by atomic force microscopy, J. Physical Chemistry B, 105 (2001). 9395-9405.

[8] T. Zama, N. Tanaka, W. Takashima, K. Kaneto, Fast and large stretching bis(trifluoromethylsulfonyl)imide (TFSI)-doped polypyrrole actuators and their applications to small devices, Polymer Journal 38 (2006) 669-677.

[9] J. Ding, D. Zhou, G.Spinks, G. Wallace, S.Forsyth, M. Forsyth, D. MacFerlane, Use of ionic liquids as electrolytes in electromechanical actuator systems based on inherently conducting polymers. Chem. Mater. 15 (2003) 2392-2398

[10] K.Yamato, W. Takashima, K. Kaneto, Stability of electrochemomechanical strains in polypyrrole films using ionic liquids, Synthetic Metals 159 (2009) 839-842.

[11] L. Bay, K. West, P. Sommer-Larsen, S. Skaarup, M. Benslimane, A conducting polymer artificial muscle with 12 % liner strain, Advanced Materials 15 (2003) 310-313.

[12] M. Kaneko, M. Fukui, W. Takashima, K. Kaneto, Electrolyte and strain dependences of chemomechanical deformation of polyaniline film, Synthetic Metals 84(1997) 795-796.

Maki Hiraoka obtained his Ph. D in Physics from the Department of Physics, Tokyo Metropolitan University in 2005. He worked as a postdoctoral research associate in the Correlated Electron Research Center (CERC), Advanced Industrial Science and Technology (AIST), Japan, till 2008. Then he became a staff researcher in Advanced Technology Research Laboratories (ATRL), Panasonic Corporation. Since 2009 he's at imec, Belgium, as Panasonic resident researcher. His main research interests are organic electronic and its application and Microsystems for biomedical applications.

Paolo Fiorini was born in Rome, Italy, in 1953. He received the degree in physics from the University of Rome, Rome in 1977. He has been active in the field of electrical and optical properties of semiconductors for many years, working at the University of Rome, where he was Associate Professor of Solid State Physics. In the recent years, he has performed research in the field of Microsystems at imec, Leuven, Belgium. His current research interest covers microfluidics for biological applications and for chip cooling.

John M. O'Callaghan is a postdoctoral researcher working with IMEC, Belgium. He obtained his degree in chemistry and PhD in materials chemistry from University College Cork, Ireland. His PhD focused on the structural characteristics of surfactant micelles and liquid crystals but has also worked in the field of pharmaceutics and drug delivery. Currently his research centers on electroactive hydrogels and polymers for use in biomedical devices and biomedical packaging.

Ichiro Yamashita graduated from Kyoto University and started materials research at Matsushita Electric Industrial Co., Lt. in 1978. In 1986, he joined the Exploratory Research for Advanced Technology, ERATO project run by the Research Development Corporation of Japan and started the structural study of flagellar rotary motor. He rejoined Matsushita Electric Industrial Co, Ltd., in 1991, and continued biophysical studies. In 1997 he proposed Bio Nano Process, a biological fabrication of nano-electron devices. In 2004, he and his colleagues succeeded in fabricating a floating gate memory using protein supramolecules. At present he is professor at the Graduate School of Materials Science, Nara Institute of Science and Technology and also principal researcher at the Advanced Technology Research Laboratory of Panasonic Corporation. He is now focusing his efforts on bio-inspired materials and micro fluidics bio-sensors.

Chris Van Hoof (M'87) is Integrated Systems Director and Program Director at IMEC in Leuven, Belgium. He received the Ph.D. degree in electrical engineering from the University of Leuven in collaboration with IMEC in 1992. At IMEC, he became successively head of the detector systems group (in 1998), Director of the Microsystems and Integrated Systems Department (in 2002) and Program Director (in 2007). His work focuses on the application of advanced packaging and interconnect technology (2D and 3-D integration, RF integration) and ultra-low-power design technology for the creation of integrated

systems, ultra-low power wireless autonomous sensor systems and smart implantable devices. His work has resulted in flight hardware for two cornerstone European Space Agency missions and he is a laureate of the Belgian Royal Academy of Sciences. Since 2000 he has also been a Professor at the University of Leuven and he is currently the promoter of eight doctoral theses.

Maaike Op de Beeck received her engineering degree in 1985 and her PhD in electronics in 1993 from the Catholic University of Leuven (KUL) in Belgium. She held several research positions at the KUL, at Philips (The Netherlands), and Mitsubishi Electric (Japan) and since 1992 she works at imec (Belgium). During the first 20 years of her carrier, she was a researcher specializing in advanced lithography. Since 2007 she became active in the field of biomedical applications. Currently she is program manager of imec's HUMAN++ program, focussing on development of Microsystems for biomedical applications. She coordinates activities in the field of Packaging and Microfluidics.